Electronic Supplementary Material (ESI) for Environmental Science: Nano.

Coupling Single Particle ICP-MS with Field-flow Fractionation for Characterizing Metal Nanoparticles Contained in Microplastic Colloids

Angie Barber[1,3], Sun Kly[2], , Matthew G. Moffitt[2], Logan Rand[1], and James F. Ranville [1*]

[1]Department of Chemistry, Colorado School of Mines, Golden, CO, 80403

[2]Department of Chemistry, University of Victoria, Victoria, B.C. V8W 2Y2

[3]Arcadis U.S., Inc., Broomfield, CO, 80021

Electronic Supplementary Information

ESI-1. Procedure for the synthesis of Au-PS NPs

The following presents the experimental procedures used for the synthesis of Au-PS NPs, which were used as a precursor for the synthesis of Au-PS-*b*-PAA NPs..

ESI-1.1. Preparation of citrate-stabilized gold nanoparticles

All glassware was cleaned thoroughly via base bath prior to use. All chemicals were obtained from (Sigma-Aldrich™) and used as purchased. Under ambient conditions chloroauric acid trihydrate was combined with deionized water to make 50 mL of a 0.01 % (w/w) solution in a 100 mL round bottom flask. In a clean sample vial, sodium citrate was dissolved into deionized water to form a 1% (w/w) solution. The solution of chloroauric acid was brought to a boil. At the first instance of boiling 0.45 ml of the 1% sodium citrate solution was added. The resulting solution turned blue after 25 seconds and red after 70 seconds. The mixture was then allowed to reflux for another 10 min, cooled to room temperature and then stored at 4°C. TEM images of freshly prepared citrate-stabilized gold nanoparticles (Au-cit NPs) were compared against those obtained after 3 days and after 1 month.

ESI-1.2. Preparation of polystyrene-stabilized gold nanoparticles

Thiol-terminated polystyrene (PS-SH, M_n = 29000 g mol^{-1}) (PDI = 1.07) (SH-Functionality >90%) was obtained from Polymer Source™. Under ambient conditions, PS-SH was combined with THF to make a 17 mg mL^{-1} solution. Au-cit NP solution was set to stir at approximately 600 rpm. The ligand exchange proceeded by drop-wise addition of 1 mL of PS-SH solution to 5 mL of Au-cit NPs allowing to stir overnight. A thin layer of purple polystyrene-stabilized nanoparticles formed atop the aqueous solution. Chloroform was added to the mixture to dissolve the thin polymer layer into a purple organic layer beneath the aqueous layer. The organic layer was collected by pipette. Particles that migrated to the water chloroform interface were purposefully not collected because they might not be fully exchanged. The PS-stabilized gold nanoparticle (Au-PS NP) solution was then transferred to a weighed vial, rotovapped to dryness, and then further dried in a vacuum oven overnight without heating to remove remaining solvent. Enough DMF was added to the dry particles to make a 1% (w/w) solution which was then stored at 4°C. TEM images of freshly prepared nanoparticles were compared against those obtained after 3 days and after 1 month.

ESI-2. Procedure for the synthesis of Au-PS-*b*-PAA NPs

The following presents the experimental procedures used for the synthesis of precursor Au-PS-*b*-PAA NPs.

ESI-2.1. Microfluidic reactor fabrication

Negative masters were fabricated on silicon wafers (Silicon Materials) using the negative photoresist SU-8 100 (Microchem). A 150 µm-thick SU-8 film was spin-coated at 2000 rpm onto the silicon wafer and heated at 65 °C for 12 min and then at 95 °C for 50 min. After cooling down the wafer, a photomask was placed over it and exposed to UV light for 100 s. Then, the UV-treated film was heated at 65 °C for 1 min and then 95 °C for 20 min. Finally, the silicon wafer was submerged in SU-8 developer (Microchem) and rinsed with isopropanol until all unexposed photoresist was removed.

ESI-2.2. Microfluidic chip preparation

Microfluidics chips were fabricated from poly(dimethyl siloxane) (PDMS) using a SYLGARD 184 silicon elastomer kit (Dow Corning). For fabrication of all PDMS chips, the elastomer and curing agent were mixed at a 7:1 ratio and degassed under vacuum. The resulting mixture was poured over a clean negative master chip in a Petri dish and further degassed until all remaining air bubbles were removed. The PDMS was heated at 85 °C until cured (~20 min), and then peeled from the negative master; holes were punched through the reservoirs of the resulting PDMS chip to allow for the insertion of tubing. A thin PDMS film (substrate layer) was also made on a glass slide by spin-coating a 20:1 elastomer / curing agent mixture followed by curing. The substrate layer was then permanently bonded to the base of the microfluidic reactor (channel layer) after both components were exposed to oxygen plasma for 45 s. The resulting reactor has a set channel depth of 150 µm and consists of a sinusoidal mixing channel 100 µm wide and a sinusoidal processing channel 200 µm wide.

ESI-2.3. Flow delivery and control

Pressure-driven flow of liquids to the reactor inlet was provided using 1 mL gastight syringes (Hamilton, Reno, NV) mounted on syringe pumps (Harvard Apparatus, Holliston, MA). The microfluidic chip was connected to the liquid syringes *via* 1/16th-inch (OD) Teflon tubing (Scientific Products and Equipment, ON). Gas flow was introduced to the chip *via* an Ar tank regulator and a downstream regulator (Johnston Controls) for fine adjustments. The chip was connected to the downstream regulator through a 1/16th-inch (OD) / 100-µm (ID) Teflon tube (Upchurch Scientific, Oak Harbor, WA). The liquid flow rate (Q_{liq}) was programmed *via* the syringe pumps and the gas flow rate (Q_{gas}) was fine-tuned *via* the downstream pressure regulator in order to dial in the nominal total flow rate of 200 µL/min. Due to the compressible nature of the gas and the high gas/liquid interfacial tension, discrepancies arise between the nominal (programmed) and actual values of Q_{gas}, $Q_{\text{gas}}/Q_{\text{liq}}$, and the total flow rate (Q_{total}). Therefore, the actual gas flow rate was calculated from the frequency of bubble formation and the average volume of gas bubbles, determined from image analysis of the mean lengths of liquid and gas plugs, L_{liq} and L_{gas}, respectively, under a given set of flow conditions. This method of flow calculation has been previously employed in the context of gas-liquid segmented flow in the microfluidic device. For the synthesis of nanoparticles described in this publication, the actual gas-liquid flow ratio and total flow rate were determined to be: $Q_{\text{gas}}/Q_{\text{liq}} \sim 1.04$ and $Q_{\text{total}} \sim 204$ µL min^{-1}.

Visualization of the gas bubbles and liquid plugs within the microfluidic reactor was achieved using an upright optical microscope (Omax) with a 10x-objective lens. Images were captured using a 2.07 megapixel PupilCam (Ken-A-Vision) and mean lengths of liquid and gas plugs were determined from the images using image analysis software (ImageJ).

ESI-2.4. Microfluidic preparation of PS-*b*-PAA composite Au-PS nanoparticles

Polystyrene-*b*-polyacrylic acid (Mn = 70k-b-13k) (PDI = 1.10) was purchased from Polymer Source™. PS-*b*-PAA was dissolved in DMF at 1% (w/w) and allowed to mix overnight. For microfluidic preparation of the composite nanoparticles three fluid streams were combined to form gas-segmented liquid plugs within the reactor: (1) 1 wt % mixture of equal parts (w/w) PS-*b*-PAA and Au-PS NP solution in DMF, (2) pure DMF, and (3) a 12 wt % solution of water in DMF. The relative flow rates of the three liquid streams, Q_{liq1}, Q_{liq2}, Q_{liq3}, respectively, were set such that combination of the streams yielded steady-state on-chip concentrations of 0.33 wt % copolymer, 0.33 wt % Au-PS NPs, and 4 wt % water. Microfluidic flow conditions were selected and controlled as described in the previous section. During collection momentary flow stoppages would occur, and during these times the outlet tube from the chip is removed from the accumulating sample until the flow becomes regular again. Samples were collected from the chip into 10x excess deionized water while stirring, and stored at 4°C. TEM images of freshly prepared composite nanoparticles were compared against those obtained after 3 days and after 1 month.

ESI-3. The following presents supplementary information about characterization methods and results for Au-cit, Au-PS, and Au-PS-*b*-PAA NPs.

ESI-3.1. Total ^{197}Au by ICP-MS

The total ^{197}Au concentration for the Au-PS-*b*-PAA NP and the Au-cit NP precursor were determined by ICP-MS analysis of triplicate 1:100 dilutions of each bulk solution (in Milli-Q water). The average signal intensity (ICP-MS counts per dwell time) was calculated for each replicate, and the concentration was calculated based on the dissolved Au calibration curve (Figure ESI-1). After adjustment for dilution, the average total Au concentration in the Au-PS-*b*-PAA NP and Au-cit NP bulk solutions is 41.754 ± 0.086 ppm and 2.753 ± 0.058 ppm, respectively.

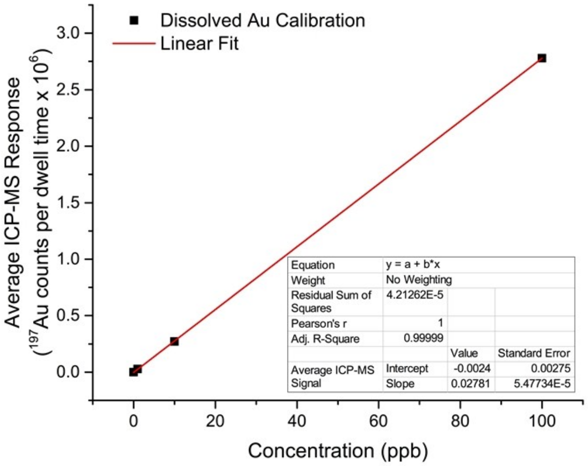

Equation	y = a + b*x		
Weight	No Weighting		
Residual Sum of Squares	4.21262E-5		
Pearson's r	1		
Adj. R-Square	0.99999		
		Value	Standard Error
Average ICP-MS Signal	Intercept	-0.0024	0.00275
	Slope	0.02781	5.47734E-5

Figure ESI-1. ICP-MS dissolved Au calibration curve for 0, 1, 10, 100 ppb Au (SPEX CertiPrep) in 2% HCl, collected for ^{197}Au using 2187.5 ms dwell time/reading and 55 readings with a 1 mL/min sample flow rate.

Table ESI-1. spICP-MS operating conditions.

Parameter Group	**Parameter**	**Condition**
ICP-MS components	Model	NexION 300D
	Mass analyzer	Quadrupole
	Nebulizer	Concentric glass, Type C (Meinhard)
	Spray chamber	Baffled glass cyclonic (PerkinElmer)
	Torch	0-Slot Quartz Torch (PerkinElmer)
	Cones	Nickel (PerkinElmer)
	Software	Syngistix^{TM} Nano Application Module (Perkin Elmer)
Data acquisition and method conditions	Nebulizer gas flow rate	0.86 – 0.98 L/min
	Sample flow rate	0.3 mL/min
	Plasma RF power	~1600 W
	Sample flush, read delay, and wash time	60 s (-24 rpm), 30-45 s (-20 rpm), 60 s (-24 rpm)
	Analytes	^{197}Au
	Dwell time	100 μs
	Scan time	60 s
	Assumed density (Au)	19.3 g/cm^3
	Mass fraction (Au)	100%
	Ionization efficiency (all)	100%
	Transport efficiency	5.89 – 10.32%
Transport efficiency and calibration standards	Particle Au (concentrations / matrix)	0 ppt and 500 ppt Au-citrate NP (NIST, 50 mg/L, 56 nm by TEM) in Milli-Q water (18.2 MΩ-cm)
	Dissolved Au (concentrations / matrix)	0, 1, 5, 10, 20, and/or 100 ppb Au$^+$ (SPEX CertiPrep, 100 mg/L, Lot # CL5-56AU) in 2% (v/v) HCl (Fisher Scientific, Optima grade, 32-35% diluted by vol. in Milli-Q water)

Table ESI-2. Summary of all spICP-MS analyses including sample and data acquisition conditions for each analysis type and sample.

Analysis Type	**Sample**	**Nebulizer Gas Flow (mL/min)**	**Transport Efficiency (%)**	**Dilution[1]**	**Analyte(s)**
spICP-MS of bulk solution	Au-PS-*b*-PAA	0.88	7.55	1x10^{4}	^{197}Au
	Au-cit	0.88	7.55	1x10^{6}	^{197}Au
	50 nm Au-cit-normal	0.93	11.42	5:1x10^{6}	^{197}Au
	50 nm Au-cit-narrow	0.89	11.50	5:1x10^{7}	^{197}Au
	100 nm Au-cit-narrow	0.93	11.42	1x10^{4}	^{197}Au
spICP-MS analysis of AF4 fractions	Au-PS-*b*-PAA 4 fractions: 12-14 min 24-26 min 32-34 min 48-50 min	0.98	6.54	10	^{197}Au
spICP-MS analysis of CFFF fractions	Au-PS-*b*-PAA	0.84 – 0.89	10.60 – 10.98	-	^{197}Au
	16 fractions:			-	
	1 (0-3 min)			0	
	2 (3-6 min)			10	
	4 (9-12 min)			0	
	5 (12-15 min)			0	
	8 (21-24 min)			0	
	10 (27-30 min)			0	
	15 (42-45 min)			8	
	17 (48-51 min)*			0	
	18 (51-54 min)*			0	
	20 (57-60 min)			12	
	22 (63-66 min)*			10	
	23 (66-69 min)*			8	
	25 (72-75 min)			3	
	27 (78-81 min)*			3	
	28 (81-84 min)*			2	
	30 (87-90 min)			0	

[1] All samples prepared in triplicate, and each triplicate sample was analyzed once, unless sufficient sample volume was not available.

* These fractions were analyzed approximately 9 weeks after the other 10 fractions. During that time, fractions were stored in 15 mL polypropylene tubes at 0-4 °C.

Table ESI-3. Summary of all field-flow fractionation analyses, including sample and data acquisition conditions, for each analysis type and sample.

AF4-UV-vis

Sample	Separation Run ID	Dilution Factor	UV-vis Wavelength (nm)	Cross-flow (mL/min)	Elution time (min)	Description
Au-PS-*b*-PAA	A	None	254	0.5	90	Initial Au-PS-*b*-PAA separation, fractions collected, no ICP-MS.
	B	1:8	520	0	6	Determined AF4 recovery by ICP-MS.
				0.5	90	
	C	None	254	0.5	90	Replicate Separation A.
	D	1:8	254	0.5	90	Replicate Separation B.
Au-cit	A	None	520	0.5	20	Initial Au-cit separation, no ICP-MS.
	B	1:10	520	0	6	Determined AF4 recovery by ICP-MS.
				0.5	20	

AF4-ICP-MS

Sample	Separation	Dilution Factor	Analyte	Dwell Time (ms)	Number of Readings	Description
Au-PS-*b*-PAA	B	1:8	^{197}Au	2187.5	275 / 2,880	Determined AF4 recovery.
Au-cit	B	1:10			275 / 750	

CFFF

Sample	Separation	Dilution Factor	UV-vis Wavelength (nm)	LS Angle	CFFF conditions	Description
Au-PS-*b*-PAA	A	0	254 and 520	90°	See text.	Separate by Au mass.
Au-cit	A	0	520	NA	See text.	

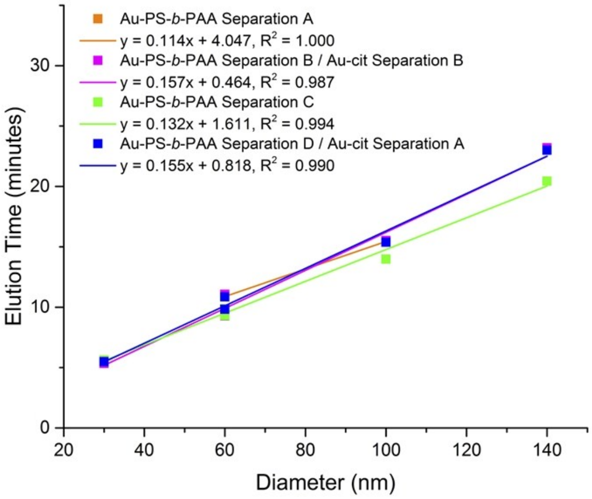

Figure ESI-2. AF4 size calibration based on retention times of 60 nm, 100 nm, and 140 nm polystyrene spheres and 30 nm and 60 nm NIST Au-citrate NPs for each day of AF4 analysis.

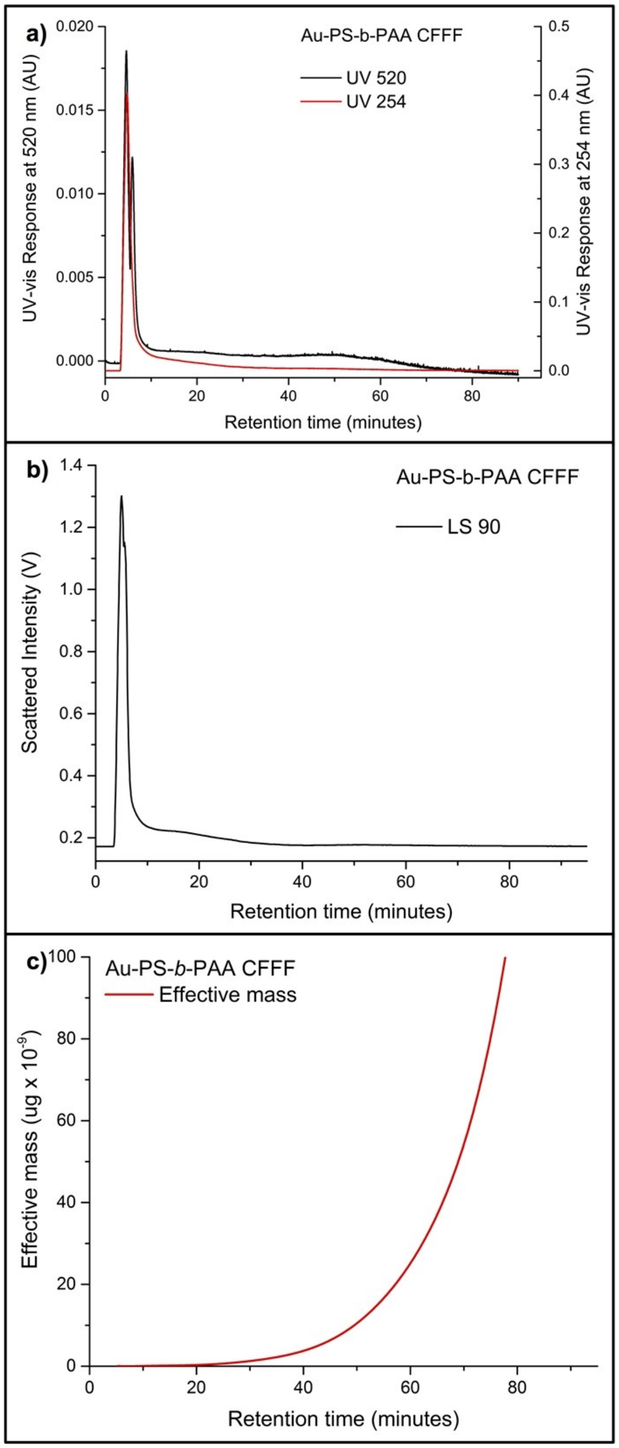

Figure ESI-3. Au-PS-*b*-PAA bulk solution was analyzed by CFFF (Postnova Analytics, Inc.) with **a)** UV-vis detection at 254 nm and 520 nm, and **b)** 90° light scattering detection. Mass versus retention time **(c)** computed by FFF theory

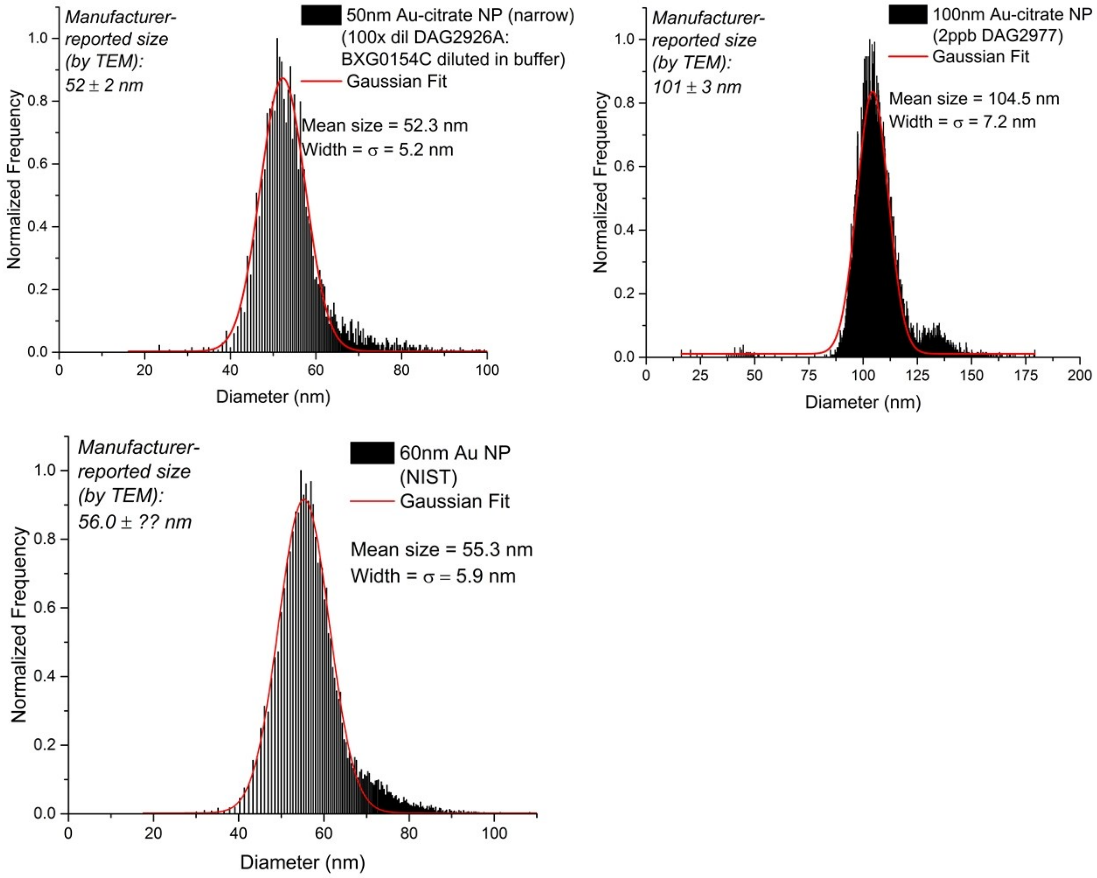

Figure ESI-4. Single particle ICP-MS results for mean diameter, uncertainty in replicate means (+/- one standard deviation), and distribution width (+/- one standard deviation around the mean) for a.) NanoComposix narrow distribution 50 nm Au-citrate NP diluted by the manufacturer, b.) Nanocomposix narrow distribution 100 nm Au-citrate NP diluted by the manufacturer, and c.) NIST reference 60 nm Au-citrate NP (RM 8013). Reported uncertainty on the mean of RM 8013 depends on the method used and ranged from 0.3-8.3.

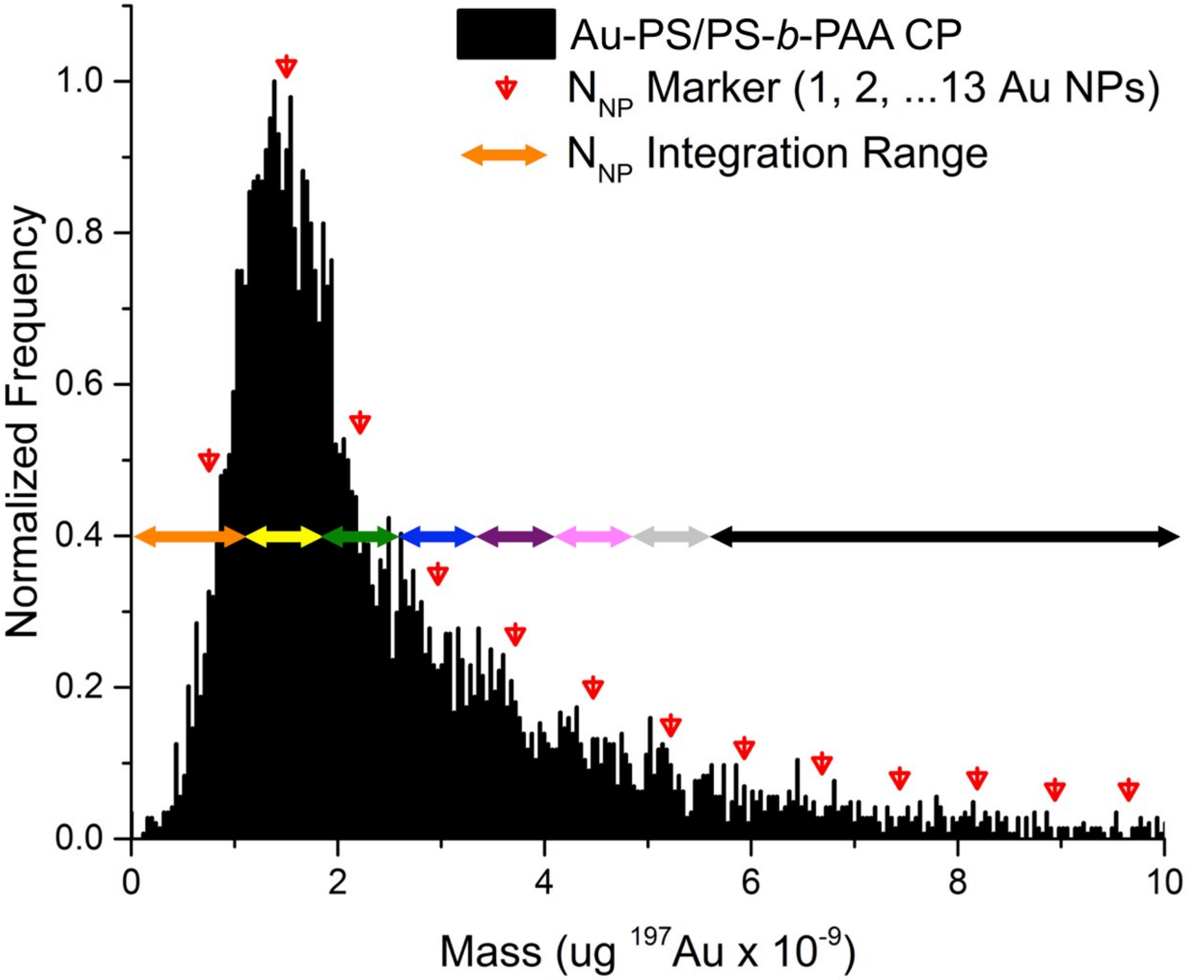

Figure ESI-5 Example using the Au-PS/PS-*b*-PAA CP sp ICP-MS data to show mass ranges (colored arrows) representing integer numbers of Au NPs contained in the CPs, established by using the mode value of 0.71 × 10^{-9} µg Au for the Au-cit particle (Figure 3a). Each range is plus and minus ½ the mass mode multiplied by an integer value of 1-8. Histograms (Figures 4 b and B) are generated by summing particle number within each range and dividing by total particle number.

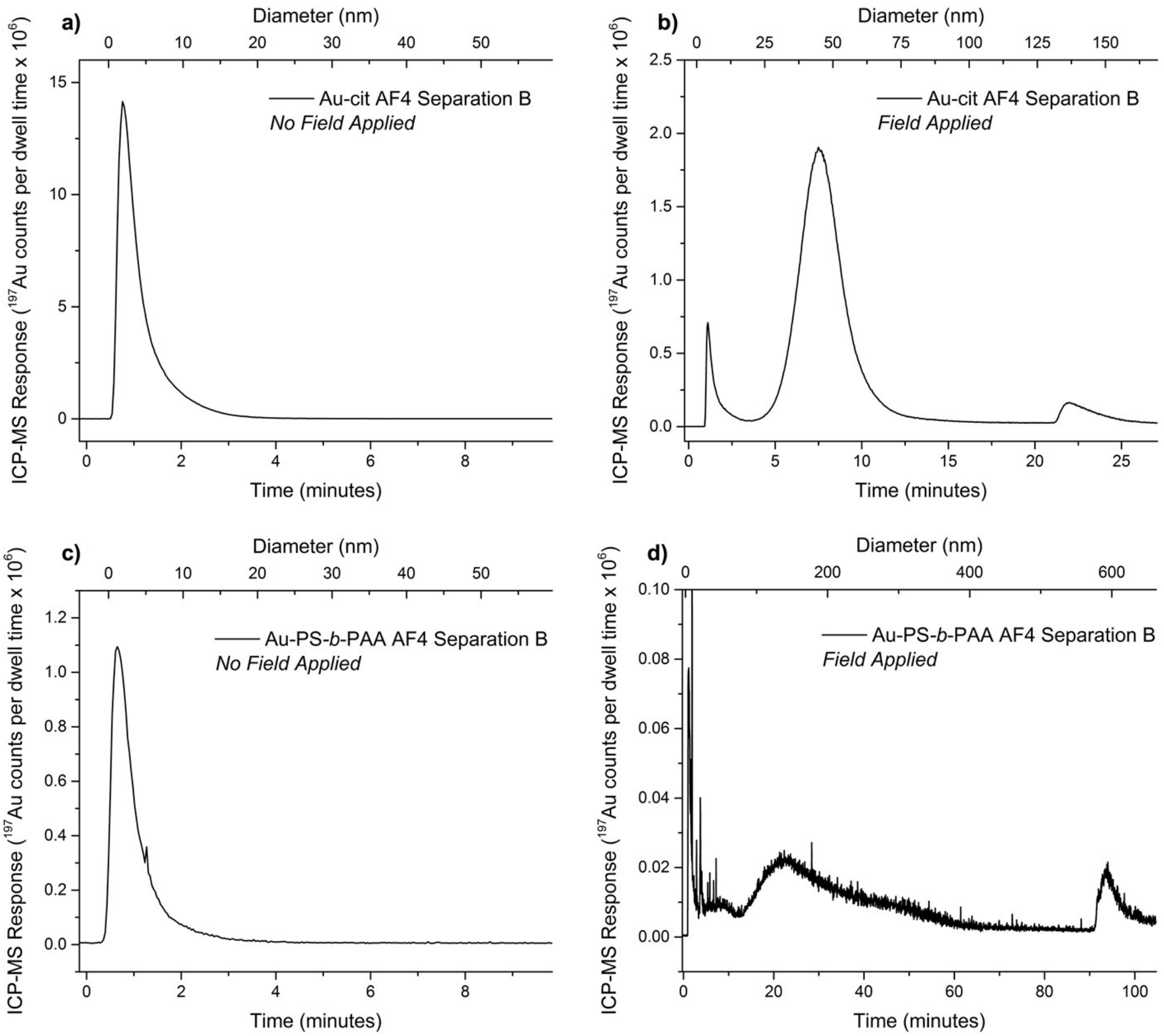

Figure ESI-6. AF4 recovery (total and resolvable) was calculated for **a-b)** the Au-cit NPs (82% and 70%) and **c-d)** the Au-PS-*b*-PAA NPs (127% and 85%) based on a comparison between the AF4-ICP-MS fractograms without an applied field and with an applied field. The field was also turned off at the end of the separations (21 minute for b. and 90 minutes for d).

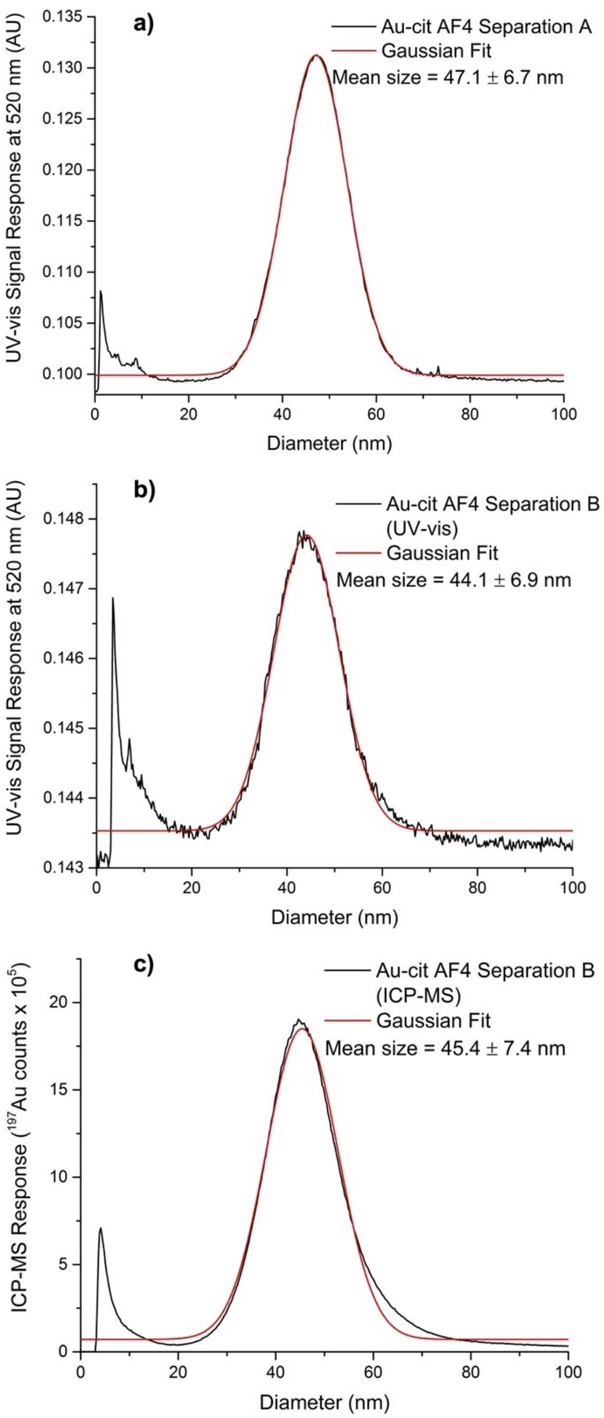

Figure ESI-7 Au-cit NP (Au-PS-*b*-PAA precursor) bulk solution was analyzed by AF4-UV-vis and AF4-ICP-MS. Conditions for Separations A **(a)** and B **(b-c)** are shown in Table ESI-3. The mean size ± standard deviation of the Gaussian fit (width) obtained with OriginPro 2015 is shown for the eluted NP peak.

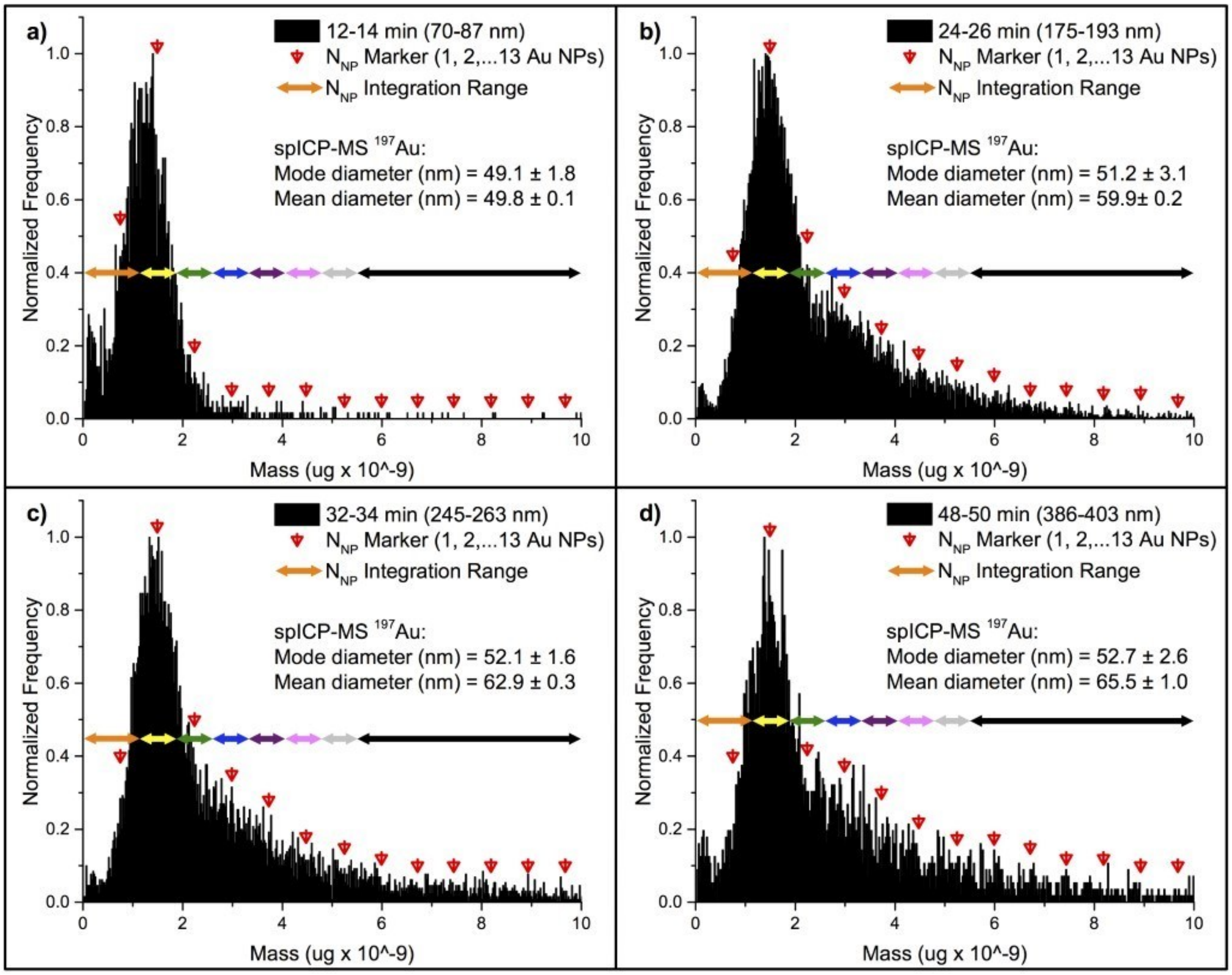

Figure ESI-8. Normalized frequency versus particle mass for four AF4 fractions analyzed by spICP-MS along with mean and mode diameters computed using Au density = 19.3 and assuming spherical geometry.

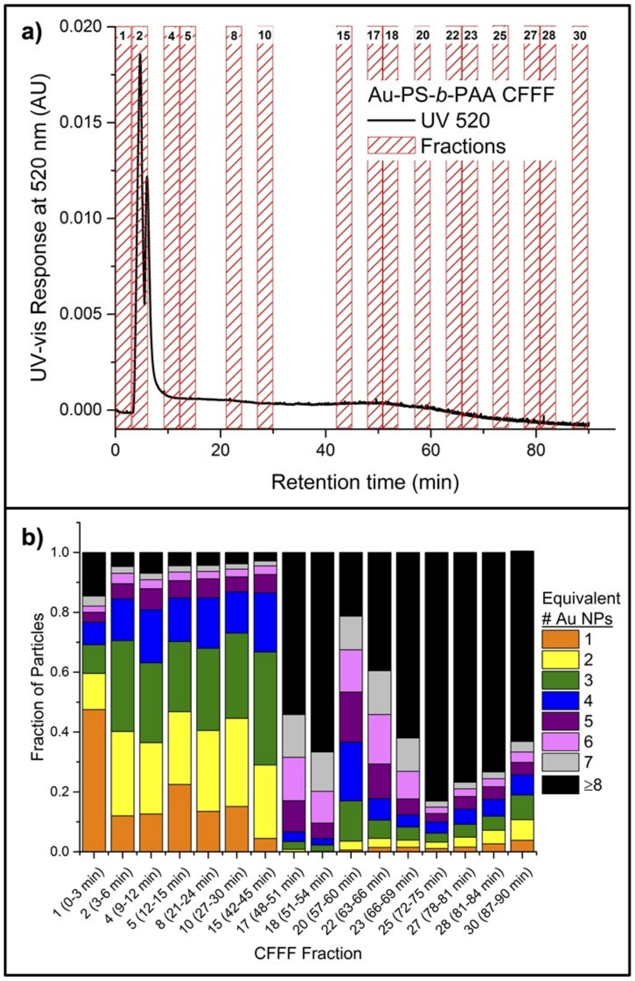

Figure ESI-9. Sixteen fractions were collected from a CFFF separation of the Au-PS-*b*-PAA sample (a). All samples were analyzed by spICP-MS and the results were binned to produce distributions of the number of particles eluting in each composite particle (b). Fractions 17,18,22,23, 27, and 28 were stored at 4^0C for 9 weeks prior to analysis and show evidence of aggregation during storage.

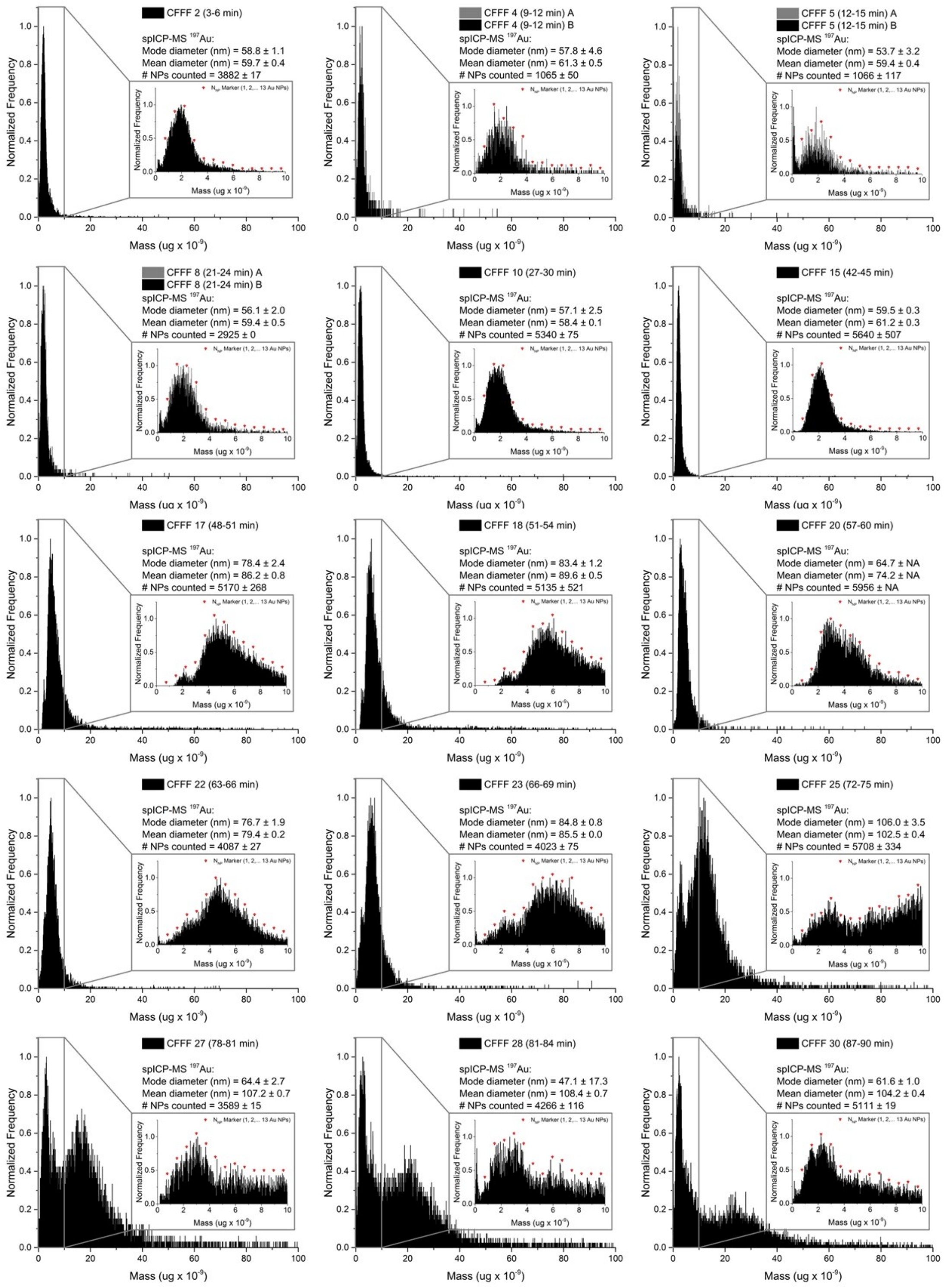

Figure ESI-10 Single particle ICP-MS normalized frequency versus particle mass for all CFFF fractions. Insets show initial part of the distribution in order to illustrate the distribution of 1-8 NPs be composite particle.